Title

Correcting spurious resolution in defocused images

ISBN

978-0-8194-6605-1

Authors

Yellott, John I

Yellott, John W

Publication Date

2007-02-15

DOI

10.1117/12.698240

Correcting spurious resolution in defocused images

John I. Yellott[a] and John W. Yellott
[a]Department of Cognitive Sciences and Institute for Mathematical Behavioral Sciences, University of California, Irvine CA 92697

ABSTRACT

Optical modeling suggests that levels of retinal defocus routinely caused by presbyopia should produce phase reversals (spurious resolution−SR) for spatial frequencies in the 2 cycles/letter range known to be critical for reading. Simulations show that such reversals can have a decisive impact on character legibility, and that correcting only this feature of defocused images (by re-reversing contrast sign errors created by defocus) can make unrecognizably blurred letters completely legible. This deblurring impact of SR correction is remarkably unaffected by the magnitude of defocus, as determined by blur-circle size. Both the deblurrring itself and its robustness can be understood from the effect that SR correction has on the defocused pointspread function, which changes from a broad flat cake to a sharply pointed cone. This SR-corrected pointspread acts like a delta function, preserving image shape during convolution regardless of blur-disk size. Curiously, such pointspread functions always contain a narrow annulus of negative light-intensity values whose radius equals the diameter of the blur circle. We show that these properties of SR-correction all stem from the mathematical nature of the Fourier transform of the sign of the optical transfer function, which also accounts for the inevitable low contrast of images pre-corrected for SR.

Keywords: phase reversal, contrast reversal, phase correction, pre-correcting defocus, presbyopia

1. INTRODUCTION: DEFOCUS AND SPURIOUS RESOLUTION

In Fourier optics the amplitude spectrum and the phase spectrum of an image are equal partners, but the optical design of the eye causes retinal images to be much more likely to suffer from amplitude distortion than from phase errors. That design makes axial defocus a routine visual event, and defocus in any image-forming device always confines its damage to spatial contrast, and has (almost) no impact on spatial phase. One way to demonstrate this is to progressively defocus the projected image of a sine wave grating, taking care to compensate for magnification artifacts. The image will fade and eventually disappear, but during this process it always remains fixed in place, never shifting laterally one way or the other along its axis. This shows that while defocus has complete power over the contrast of the image, it cannot produce any shift in its spatial phase. Such a limitation might be expected *a priori* from symmetry considerations together with the one-dimensional nature of defocus, which is essentially a distance error in the positioning of the image-observation plane along the z-axis of the optical system. That z-axis error provides no basis for shifting the image of a spatial sine wave laterally in the x,y plane, because it does not imply a choice of one direction over the other.

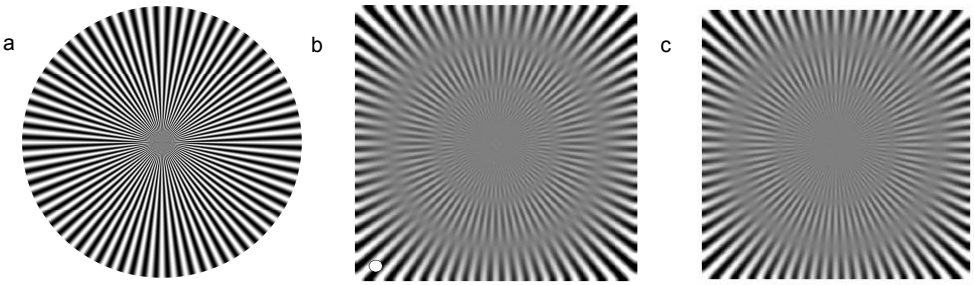

Fig. 1. Spurious resolution and its correction. *a*: sinusoidal version of Siemen's star[3]: $cos72\theta$. *b*: image *a* after convolution with a uniform disk, simulating optical defocus. The size of the blur-disk is shown by a white spot in the lower left corner. *c*: image *b* with its phase spectrum corrected to undo spurious resolution.

Human Vision and Electronic Imaging XII, edited by Bernice E. Rogowitz, Thrasyvoulos N. Pappas, Scott J. Daly, Proc. of SPIE-IS&T Electronic Imaging, SPIE Vol. 6492, 64920O, © 2007 SPIE-IS&T · 0277-786X/07/$18

So defocusing a grating down to its first disappearance yields no surprises. But now if the defocusing process is continued beyond the point of zero contrast, one may be surprised to find that the image reappears, only with reversed contrast—dark stripes in the object become light stripes in its image, and light stripes turn dark. This phenomenon is known as "spurious resolution" [1] (SR). Fig. 1 shows a classic demonstration [2,3], to which we have added a new wrinkle by showing what happens when SR is corrected. Here, the visual result is subtle, but for other images it can be dramatic.

Another name for spurious resolution is "phase reversal"[4]. That name is prompted by the fact that from a Fourier perspective, these contrast reversals are actually phase changes—half-cycle phase shifts, which leave a spatial sine wave in place, but reverse its sign: $a \cos 2\pi f(x + 1/2f) = -a \cos 2\pi fx$. This is the only phase change that defocusing can produce—the only exception to the rule that defocus cannot alter phase. It satisfies the demands of symmetry by being the only phase change that does not entail choosing sides.

So during the eye's constant struggle to stay in focus, SR is the only phase error that can occur when it fails. It is natural to wonder what visual effect such errors have, and what would happen if they could be corrected. This paper deals with these questions. Our interest is specifically motivated by the fact that SR admits the possibility of being pre-corrected in visual targets (e.g., printed letters) by shaping them in a way that anticipates the phase reversals to be expected from subsequent defocus (e.g., by a presbyopic eye), and uses them to create recognizable retinal images of the original forms. The rest of this section provides a mathematical framework for the analysis. Section 2 examines the potential visual impact of SR during out-of-focus reading, which proves to be substantial. Section 3 shows that correcting SR in severely blurred letter-images can restore them to legibility, and that the effectiveness of this correction is remarkably independent of the extent of defocus. We show how these properties of SR-correction arise from the nature of the change it produces in the defocused pointspread function, and how that the nature of that change stems in turn from properties of the Fourier transform of the sign of the corresponding optical transfer function. Finally, Section 4 considers the possibility of achieving the benefits of SR-correction during presbyopic vision by re-shaping printed text in a way that should—in theory—cause a defocused eye to correct its own phase error. We show that such pre-corrections are fundamentally limited by contrast constraints imposed by the basic nature of the operation. We use computation and mathematical analysis to map out this territory, which is part of a still largely mysterious domain: the role of phase in visual images. Our goal is develop an intuitive mathematical understanding—a geometrical picture--of how SR-correction works on images and their spectra, so that its effects can be anticipated, rather than having to be freshly computed for each situation.

1.1 Mathematics of spurious resolution

$o(x,y)$ denotes the light intensity in a monochromatic object; $i_o(x,y)$ is the intensity in its image; x and y are visual angle coordinates, with axes are labeled so that (x,y) in the image plane is the geometrical optics image of (x,y) in the object plane. $Fo(u,v)$ and $Fi_o(u,v)$ are the Fourier transforms of o and i_o; u and v are cycles/unit visual angle. We consider a shift-invariant linear optical system with pointspread function $p(x,y)$: p is the image of the point object $\delta(x,y)$. The functions o, i_o, and p are all real and nonnegative; p is assumed to have volume 1.0. The system is completely characterized by p through the convolution relationship $i_o(x,y) = o(x,y) * p(x,y)$. In the spatial frequency domain the same characterization is represented by the product relationship $Fi_o(u,v) = Fo(u,v)\ Tp(u,v)$, where Tp is the Fourier transform of p: Tp is the optical transfer function (OTF) of the system. In exponential form $Tp(u,v) = |Tp(u,v)|\ exp[j\Phi p(u,v)]$, where the modulus $|Tp(u,v)|$ is the amplitude spectrum portion of the OTF (i.e.., the modulation transfer function), and the argument $\Phi p(u,v)$ is its phase component—the phase transfer function corresponding to the pointspread p. $|Tp| \geq 0$, of course, and because p is real, $|Tp(-u,-v)| = |Tp(u,v)|$ and $\Phi p(-u,-v) = -\Phi p(u,v)$. Those relationships hold for any system, but if we assume in addition that the optical system is limited only by factors that produce a radially symmetric pointspread function (in particular, defocus, but also diffraction by, e.g., a clear circular pupil), then Φp becomes tightly constrained: radial symmetry in p (i.e., $p(-x,-y) = p(x,y)$) implies radial symmetry in Tp, so

$$|Tp(-u,-v)|exp[j\Phi p(-u,-v)] = |Tp(u,v)|exp[j\Phi p(u,v)]\ . \qquad (1)$$

Combining that relationship with the other two, we have $exp[-j\Phi p(u,v)] = exp[j\Phi p(u,v)]$. This can only be true if

$\Phi p(u,v) = n\pi$ for some integer n, so the only possible values of the phase transfer function $exp[j\Phi p(u,v)]$ are +1 and −1. Consequently the OTF imposed by defocus is always real, and takes the form

$$Tp(u,v) = |Tp(u,v)|\ Sign[Tp(u,v)] \tag{2}$$

where $Sign[x] = 1$ for $x > 0$, −1 for $x < 0$, and 0 at $x = 0$. This representation of the defocused OTF is the key to understanding spurious resolution and its correction. SR occurs at exactly those spatial frequencies (u,v) where $Sign[Tp(u,v)] = -1$; whenever this is true, Tp introduces its only possible phase error: a reversal of contrast-sign . We can correct this defect of Tp by multiplying it times its own sign, turning it into $|Tp|$:

$$Tp(u,v)\ Sign[Tp(u,v)] = |Tp(u,v)|\ Sign[Tp(u,v)]\ Sign[Tp(u,v)] = |Tp(u,v)| . \tag{3}$$

So to correct the phases in the image i_o of an object o that has been blurred by defocus, we multiply its spectrum Fi_o times the sign of the OTF Tp, producing a new, phase-corrected, spectrum, denoted Fci_o , whose phase component is the same as that of the object spectrum, and only differs from it only in amplitude:

$$Fci_o(u,v) = Fi_o(u,v)\ Sign[Tp(u,v)] = Fo(u,v)\ Tp(u,v)\ Sign[Tp(u,v)]$$

$$= Fo(u,v)\ |Tp(u,v)| = |Fo(u,v)|\ |Tp(u,v)|\ exp[j\Phi o(u,v)]. \tag{4}$$

The phase-corrected image that results from this operation, $ci_o(x,y)$, can be obtained by taking the inverse Fourier transform of Fci_o. One such image was shown in Fig. 1*c*. In that case the immediate visual impact of SR correction was small. But for other objects the effect can be visually dramatic (Fig. 6) and intellectually surprising (Fig. 7).

Note that the SR-correcting multiplication (4) can be performed directly on the object spectrum rather than on the spectrum of its image. In that case we can create a pre-corrected version of object o, denoted $co(x,y)$, whose transform $Fco(u,v)$ is the product $Fo(u,v)\ Sign[Tp(u,v)]$. Then when imaging has its usual effect of multiplying the object spectrum times Tp, the result will be $Fo\ Sign[Tp]\ |Tp|\ Sign[Tp] = |Fo|\ |Tp|\ exp[j\Phi o]$. So defocusing the object co leaves the original object phase spectrum Φo unchanged, and reproduces o with only the loss of contrast imposed by the modulation transfer function $|Tp|$. Such pre-corrected objects are, in effect, inoculated against spurious resolution. The pre-corrected object $co(x,y)$ itself can be created by Fourier inversion of its spectrum $Fco(u,v)$. However as we will see, the actual physical realizability of co is problematic, because the theoretical image produced in this way generally contains negative values, and these prove to impose severe constrains on the retinal contrast of SR-corrected images.

2. SPURIOUS RESOLUTION IN PRESBYOPIC VISION

Besides being useful for demonstrating SR with a slide projector, the star pattern in Fig.1*a* can be used to investigate whether SR occurs in out-of-focus human vision, by viewing it very close to one's own eye--too close to focus. (An inch or two should do. If the video image of the star has become distorted in this copy, a printed version may still be OK.) Such experiments generally convince observers that SR does occur in defocused eyes, though astigmatism and other aberrations yield a visual experience that is not so clear cut as Fig. 1*b*. Psychophysical evidence on this point is surprisingly scarce and somewhat equivocal[1,4–7]; results depend on what is demanded of observers in an experiment, and on parameters such as pupil size and the sign of defocus. But it seems quite clear that SR would be expected on optical grounds if the eye were a perfect device, limited only by defocus plus diffraction at the pupil, and that it should play an important role in vision at levels of defocus that are commonly experienced by many people in daily life. Figure 2 shows an analysis of a bare-bones model of a human eye that is correctly focused for infinitely distant objects, but has no ability to refocus for nearer ones, like older people who are completely presbyopic and require +3 diopter reading glasses. The figure shows the pointspread function and the OTF of this eye when viewing incoherent monochromatic objects at infinity (in the upper half of the figure) and at 30 cm (lower half). The in-focus pointspread is the Airy pattern (on this scale, visible only as a dot) with a central spot about 1 min across; its OTF is monotonically decreasing, and vanishes around 90

cycles/deg. When the object point moves in to 30 cm, producing 3.3 diopter defocus, its image becomes a broad flat cake with ripples, about 1/2 degree in diameter. (Fig. 3*a* below shows the profile of this pointspread function.)

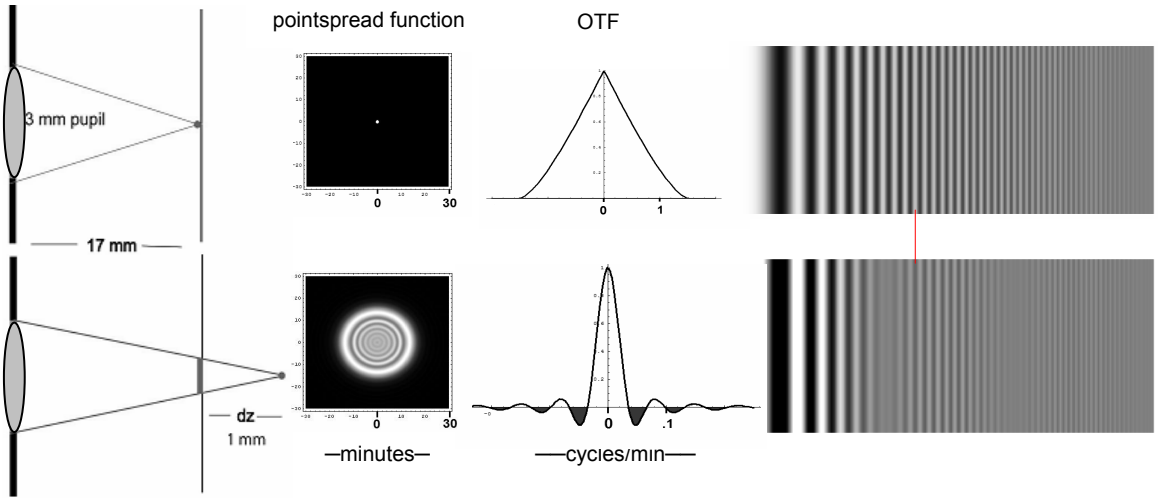

Fig. 2. Spurious resolution created by defocus in a model eye. 3 mm circular pupil, thin lens focal length = retinal distance = 17mm, monochromatic 550 nm point object. *Upper row*: object at ∞; no defocus, OTF due to diffraction alone. *Lower row*: object at 30 cm, OTF due to diffraction plus defocus (3.3 diopters) . OTFs and point spreads based on Hopkins[9,10]; at 30 cm the wavefront error w_{20} is -6.7λ. The Strehl ratio here is around 10^{-3}. Panels on the right show a sweep-frequency grating before and after defocus. The line | marks a stripe whose contrast is reversed by SR.

The OTF now has its first zero at 2 cycles/deg and remains negative up to 4 cycles/deg, so all spatial frequencies in this range will be imaged with reversed contrast. This should have a significant impact on reading, which depends critically on the visibility of frequencies that correspond to around 2 cycles/letter[8]. A 10-point letter at 30 cm subtends 2/3 deg, so 2 cycles/letter here corresponds to 3 cycles/deg, the center of the first spurious resolution range. Lower levels of defocus push that range up to higher frequencies (e.g., for 2D defocus with a 3 mm pupil, SR begins at 3.5 cycles/deg) but larger pupil sizes push it down (for a 6mm pupil, SR begins at 1.8 cycles/deg for 2D) . Overall, there appears to be a sizable parametric range where SR might be expected to affect presbyopic reading by reversing the contrast of critical spatial frequencies. Section 3 examines the effect this could have on the legibility of text. For that purpose it is useful to be able to model defocus using a simple uniform disk to represent the pointspread function--the geometrical optics approximation--rather than the analytically complicated pointspread implied by scalar diffraction theory[2,9,10]. The remainder of this section deals with the validity of this approximation.

2.1 Geometrical optics versus scalar diffraction theory models for visual defocus

Panel *b* in Fig. 3 compares the OTF produced by 3.3 diopter defocus in the model eye of Fig. 2 when the pointspread function is the one implied by diffraction theory (the rippled-cake shown here in Fig.3*a*) with the OTF produced by a uniform-disk pointspread function chosen to create the same first zero-crossing in the OTF. One can see that these two OTFs are nearly identical out to their third zeros, so for this level of defocus, geometrical optics provides a close approximation to diffraction optics. (Panel *c* shows how uniform-disk defocus affects the sweep-frequency grating used in Fig. 2.) Figure 4 shows similar comparisons for 1, 2, and 0.3 diopters of defocus. For 1 and 2 diopters the geometrical optics approximation retains its validity. When defocus falls below 1 diopter the diffraction OTF undergoes a qualitative change, and the geometrical optics approximation fails. Below about 0.3 diopters the diffraction OTF ceases to have any negative regions, so at low levels of defocus SR no longer occurs at all. (At these levels the pointspread function is roughly bell-shaped, and could be adequately modeled by a Gaussian. But Gaussian pointspread functions always have nonvanishing Gaussian OTFs, so whenever SR actually occurs in vision, Gaussian pointspread models cannot account for it.)

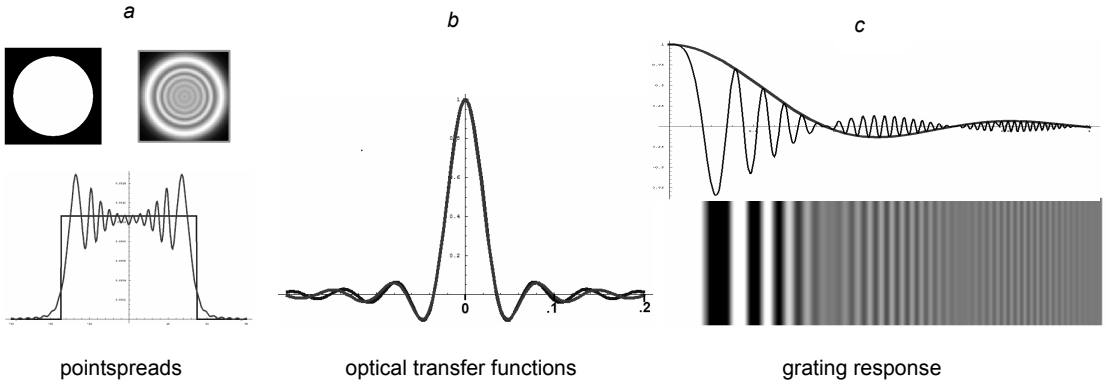

Fig.3 Comparison of geometrical optics and diffraction optics models for the 3.3 D defocused eye in Fig.2. *a*: *p*ointspread functions. The geometrical pointspread is a uniform disk with volume 1.0 and diameter 33 min. *b*: OTFs. *c*: grating response for uniform-disk defocus (blur disk shown in the lower right corner). The diffraction model response (Fig. 2) is indistinguishable from the one here.

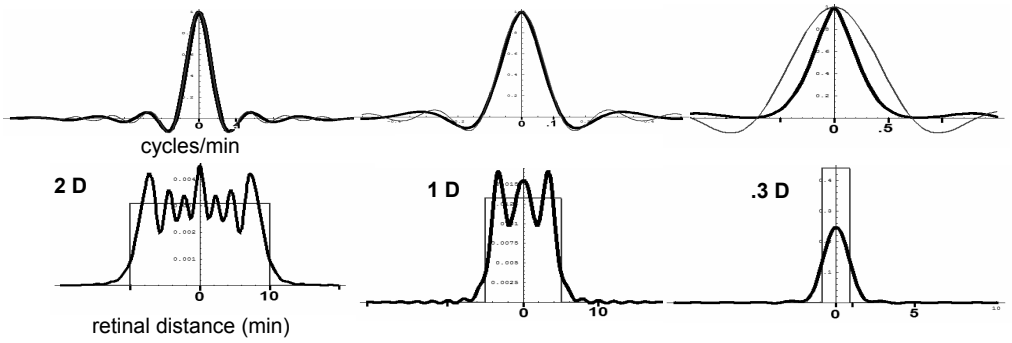

Fig. 4 Comparison of geometrical vs.diffraction models for 2, 1 and .3 diopters of defocus in the model eye of Fig. 2. *Upper row*: OTFs *Lower row*: pointspread functions. Diffraction model predictions are the thick lines.

3. EFFECT OF CORRECTING SPURIOUS RESOLUTION

Section 1.1 showed that correcting SR in a defocused image $i_o(x,y)$ is computationally straightforward, provided we know the sign of the OTF *Tp*. In that case we multiply the image transform $Fi_o(u,v)$ times the function *Sign[Tp(u,v)]*, and take the Fourier inverse of the product; the result is the phase-corrected image $ci_o(x,y)$, which differs from the original object *o(x,y)* only in its amplitude spectrum: $Fci_o(u,v) = |Fo(u,v)||Tp(u,v)|exp[j\Phi o(u,v)]$, where Φo is the phase spectrum of *o*. But what this SR-corrected image will look like is not so obvious. Fig. 1 already showed that for some objects the change produced by SR correction is quite inconspicuous, and can only be detected by close inspection. Fig. 5 shows another example of this using a sweep-frequency grating. These demonstrations are consistent with psychophysical experiments showing that phase reversals can have little impact on the perception of natural scenes[4].

But for other visual objects, SR correction can have a profound effect, turning hopelessly blurred images into easily recognizable low-contrast versions of their objects. This is notably true of printed letters; Fig. 6 shows an example . To appreciate the visual significance of this demonstration, suppose the letters in Fig. 6*a* correspond to 10 point

type viewed at 30 cm. Then their retinal images are on the order of 2/3 deg, giving the blur disk in 6*b* a diameter around 1/3 deg. In our model eye that pointspread diameter corresponds to 2 diopters of defocus (Fig. 4). So the

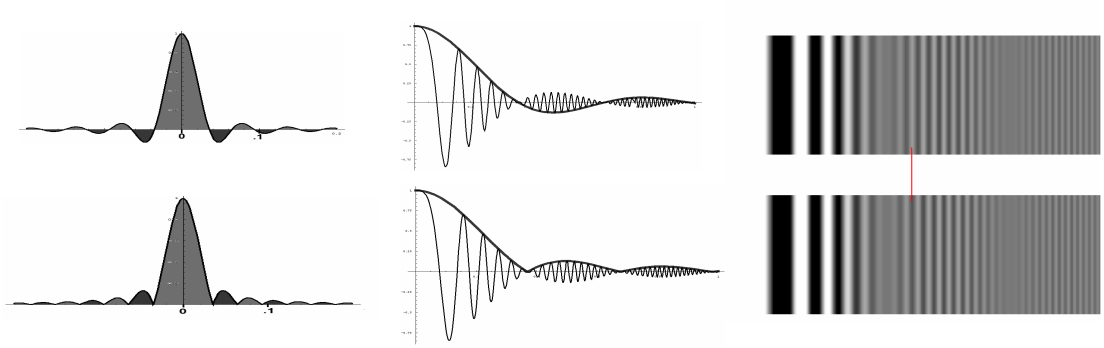

Fig. 5. Effect of correcting SR in a defocused sweep-frequency grating. The *upper row* shows the grating (from the top right of Fig. 2) after convolution with a uniform disk; the corresponding OTF (from Fig. 3) is on the left. SR correction is equivalent to rectifying that OTF, forming the nonnegative OTF shown in the *lower row*. This produces the phase-corrected grating response shown there. The thin line marks a stripe whose contrast-sign was erroneously reversed by defocus; SR correction restores the proper sign.

devastating effect of defocus seen in 6*c* would be a routine visual experience for people who normally rely on reading glasses in the 2 diopter range, whenever they try to read without them. Glasses, of course, simultaneously correct both the contrast losses and phase changes created by defocus. The dramatic improvement in letter readability produced here by correcting SR alone (Fig. 6*d)* indicates that the impact of presbyopic defocus on reading may be mainly due to phase errors. Others have come to the same conclusion[11]. So reading glasses that correct phase alone--if such things could be made—might work fairly well.

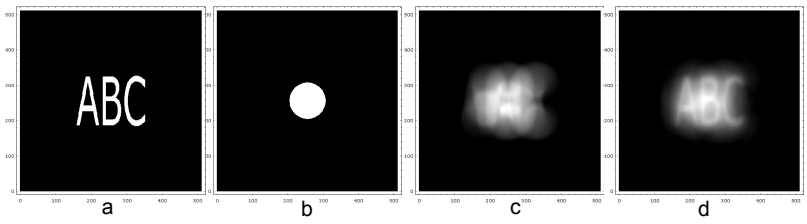

Fig 6. Effect of correcting SR in defocused letters. *a* is the original image; *b* is the blur-disk. Panel *c* shows the defocused letters, i.e., image *a* convolved with blur-disk *b*. Panel *d* shows image *c* after SR correction.

3.1 Effect of defocus severity on SR correction

Demonstrations showing that correcting SR can restore the legibility of defocused letters are not new[11]. But exploring this effect systematically reveals a remarkable property that does not seem to have been previously noted: the visual effectiveness of the correction is independent of the amount of defocus. Figure 7 shows the results of defocusing letters with blur-disks of increasing size, and then correcting the blurred image for SR. Defocus quickly makes the letters illegible, but their SR-corrected images remain completely legible for blur-disks of every size. For them, the only effect of increasing defocus is reduced contrast; the legibility of the letters is not impaired at all, but they appear to be veiled by an increasingly bright luminous fog.

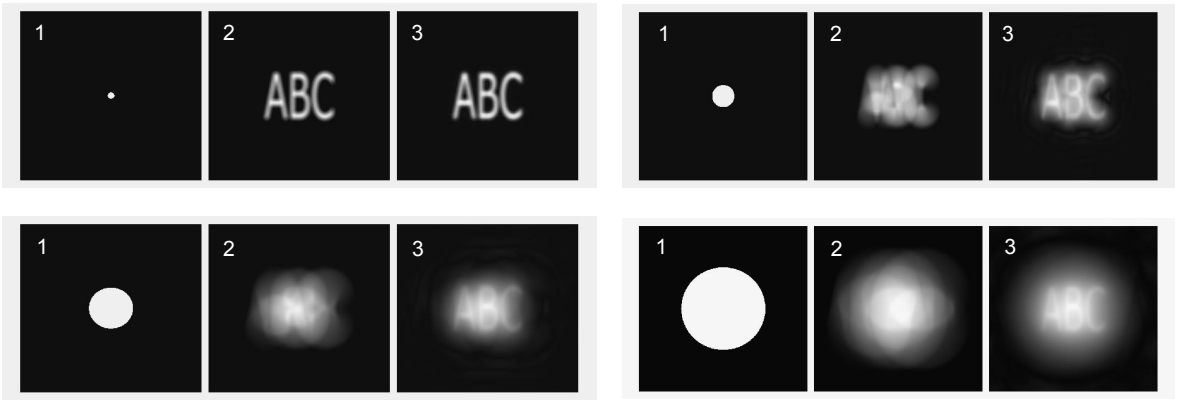

Fig. 7 Effect of correcting spurious resolution in letters blurred by increasing amounts of defocus. In each series panel 1 is the blur disk; panel 2 shows the letters after convolution with that disk; and panel 3 shows the result of correcting the phase reversals in image *2*.

3.2 SR-corrected pointspread functions

To understand the effect of SR correction on defocused letters, we start by examining its effect on single points. Using the notation of Section 1.1, correcting SR in images formed by a defocused optical system with OTF *Tp* (i.e., multiplying Fi_o times *Sign[Tp]*) is equivalent to changing the system OTF from *Tp* to |*Tp*|. This OTF has its own pointspread function, denoted *cp(x,y)*, which can be found by taking the Fourier inverse of |*Tp*|. We will use **FT***[f]* to denote the Fourier transform of a function *f*: **FT***[f(x,y)](u,v) = ∬ f(x,y) exp[-j2π(ux+vy)]dxdy* (∬ stands for integration over the whole plane). Its inverse $\mathbf{FT}^{-1}[F](x,y) = \iint F(u,v)\, exp[j2\pi(ux+vy)]\, dudv$. Then $cp(x,y) = \mathbf{FT}^{-1}[|Tp|]$ is the pointspread function of the SR-corrected system, and the corrected image of any object *o* is the convolution $o * cp$. In particular, of course, *cp(x,y)* itself is the SR-corrected image of the point object *δ(x,y)*. Figure 8 shows SR-corrected pointspread functions for both the geometrical-optics and diffraction-optics models of the 3.3 D defocused eye analyzed earlier in Fig. 2. Direct comparison (in Fig. 8*f)* shows that the two functions

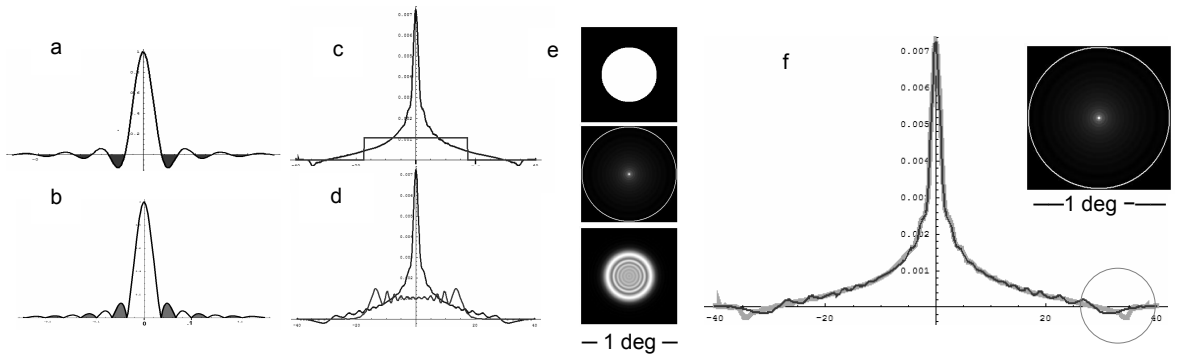

Fig. 8. Effect of SR correction on pointspread functions. *a* and *b* show the pre-and post-correction OTF of the defocused model eye in Fig. 2 (the geometrical optics version). *c* and *d* show profiles of the pre-and post-correction pointspread functions for the geometrical optics model (*c*) and the scalar diffraction model (*d*); top-down views of those functions are shown in column *e*. The middle panel in *e* is the SR-corrected geometrical pointspread; the diffraction version is indistinguishable. *f* shows a direct comparison of the two SR-corrected pointspeads; the negative light-intensity region around radius 30 min is circled, and indicated by a light ring in the top-down view (*f* inset).

are practically identical. We see that correcting SR here has the effect of changing the pointspread function from a broad flat cake (with ripples in the diffraction version) to a sharply pointed cone—like a sagging tent supported by a single pole. Fig. 8 also shows that both corrected pointspread functions have a narrow circular annulus of negative values at a radius of about ½ deg—the width of the blur disk. These "negative light" intensities are not computational artifacts, but rather constitute an intrinsic feature of the SR-corrected pointspread function. That is , for both the geometrical-optics and diffraction-optics forms of the defocused OTF *Tp*, the function $cp(x,y) = \mathbf{FT}^{-1}[|Tp|](x,y)$ really is distinctly negative within a narrow annular ring in the *x,y* plane. (Section 3.3 shows why this must be so.) This effect is numerically small, but theoretically significant. It means that a pure phase-only correction of spurious resolution phase-errors is physically impossible, because the SR-corrected pointspread function *cp(x,y)* cannot be exactly represented by a pattern of non-negative light intensities. Of course in practice we can display a facsimile of *cp* by adding a uniform background to it (as we do here), and an image of the form *cp(x,y) + constant* retains the phase-corrected property of *cp*. As illustrated by Fig. 8 (and Fig. 9 below), the constant here is generally quite small, so adding it does not produce any significant distortion.

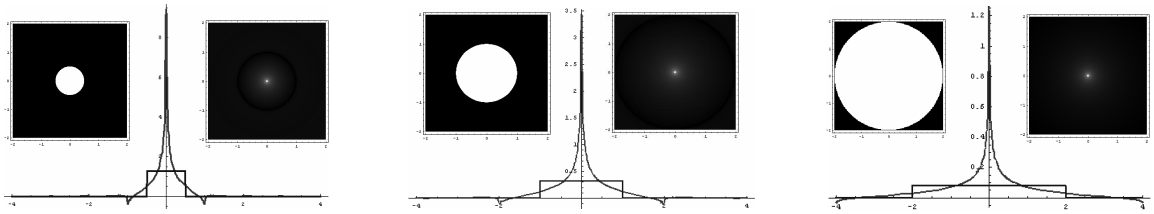

Fig. 9 SR-corrected pointspread functions for blur-disks of increasing size (diameters 1:2:4). The y-axes are on different scales: the peak response value for the largest disk would actually be 1/16 the value for the smallest disk. Both pre-and post –correction pointspeads always have volume 1.0.

Figure 9 shows how increasing the size of the blur-disk affects the SR-corrected pointspread function. One can see that for all disk sizes—all levels of defocus--the corrected pointspread always retains its sharp central spike, and the ring of negative light intensity values always has a radius equal to the blur-disk diameter. This behavior would be expected from scaling considerations: resizing the unit-volume pointspread function *p(x,y)* by a width factor *w* means changing it to $p(x/w, y/w)/w^2$, so the form of the OTF at all scales is $\mathbf{FT}[p(x/w,y/w)/w^2] = Tp(wu,wv)$. The SR-corrected OTF then is $|Tp(wu,wv)|$, and taking $\mathbf{FT}^{-1}$ of this to create the SR-corrected pointspread yields $cp(x/w,y/w)/w^2$. So changing the magnitude of defocus by altering the width of the blur-disk cannot alter the basic form of the SR-corrected pointspread function: it always consists of a sharp spike at the origin surrounded by a fringe of scattered light, with a negative ring at a radius equal to the blur-disk diameter. (Of course for the diffraction model the pointspread function does not actually have an abrupt edge. But for these high levels of defocus, its edge is sharp enough to justify this way of describing things.) When this corrected pointspread is convolved with an object to create the SR-corrected version of its defocused image, its effect is dominated by its central spike, which acts like a $\delta(x,y)$ impulse by accurately reproducing the spatial form of the object (i.e., $o * \delta = o$), with an overall amplitude reduction proportional to $1/w^2$. To this low intensity copy of the object, the broad fringe of the corrected pointspread function adds a veil of light whose intensity also proportional to $1/w^2$. So the ratio of the central spike to its own background can be expected to remain constant, independent of the blur-disk width *w*, i.e., independent of the severity of defocus. Of course for an object composed of several points the effective background will be the sum of all their fringes, and the extent of overlap will depend on the amount of defocus; so contrast can be expected to suffer somewhat as defocus increases.

3.3 Understanding the SR-corrected pointspread function

The corrected pointspread function *cp(x,y)* has two main properties: (1) its basic shape, consisting of a tall sharp spike at the origin surrounded by rapidly tapering fringe; and (2) a narrow ring of negative intensity values whose radius equals the diameter of the blur-disk correspond to the uncorrected defocused pointspread *p(x,y)*. To understand how these properties arise mathematically, we consider the operation that creates *cp*: $\mathbf{FT}^{-1}[\,|Tp|\,]$. The

true functional form of the OTF of a defocused diffraction-limited optical system is a very complicated object[9,10] involving infinite sums of Bessel functions of all orders, and taking its absolute value makes the mathematical situation worse, since that loses the resources of analytic function theory. Fortunately, for the levels of defocus that concern us here, computational comparisons (Figs. 3,4, 8) show that we can use the geometrical optics approximation of this function, which is much simpler. The pointspread function for a blur-disk of width 1.0 is the circularly symmetric function $p(x,y) = p_1(r) = (4/\pi)\ rect(r)$, where $r = (x^2 + y^2)^{1/2}$ and $rect(r) = 1$ for $|x| \le 1/2$ and $= 0$ *for* $x>1/2$. ($4/\pi$ makes the volume 1.0.) The corresponding OTF is $T_{p1}(q) = \mathbf{FT}[\ p1(r)] = (4/\pi)\ jinc(q)$, where $q = (u^2 + v^2)^{1/2}$ and $jinc[q] = J_1(\pi q)/2q$. The Fourier (Hankel) transform relationship $rect(r) \leftrightarrow jinc(q)$ is very well understood[12] , and $jinc[q]^2$ is also well known: its Fourier transform is the Airy pattern—the diffraction-limited image of a star. But the object we need is the Fourier transform of $|jinc(q)|$, which appears to be unknown. Specifically, the function cp_1 that we need to understand is defined by

$$cp_1(r) = \mathbf{FT}^{-1}[|Tp1(q)|](r) = \mathbf{FT}^{-1}[(4/\pi)\ |jinc(q)|\ )](r) = (4/\pi)\ \{\ 2\pi \int_0^\infty |jinc(q)|\ J_0(2\pi qp)\ q\ dq\ \}. \qquad (5)$$

(The profile of $cp_1(r)$ is shown in Fig. 9.) The integral expression inside the braces in (5) is the Fourier transform of |jinc(q)|. We have not been able to find an explicit solution for this integral, and the absolute value property makes it seem unlikely that such an expression can be found. Computation (and no doubt a little analytic thought) shows that it diverges (slowly) for $r = 0$, so the SR-corrected pointspread function $cp_1(r)$ is infinite at the origin, which accounts for its impulsive nature—its δ-like effect when convolved with object functions. (In a real optical device, diffraction would prevent this infinity by imposing a finite upper limit on the integral in (5).) But apart from this, (5) provides no obvious insight into the properties of $cp_1(r)$, *or* $cp(x,y)$ in general.

In search of that, we try another approach, based on the fact that cp is the convolution of the pointspread p and the function $\mathbf{FT}^{-1}[Sign[Tp]\ ]$. That relationship follows from the product representation of $|Tp|$ in Eq.3 :

$$cp = \mathbf{FT}^{-1}[\ |Tp|\ ] = \mathbf{FT}^{-1}[\ Tp\ \ Sign[Tp]\ \ ] = \mathbf{FT}^{-1}[Tp\ ] * \mathbf{FT}^{-1}[\ Sign[Tp]\ ] = p * \mathbf{FT}^{-1}[\ Sign[Tp]\ ] \qquad (6)$$

For our special case, $cp_1(r) = p_1(r) * \mathbf{FT}^{-1}[\ Sign[jinc(q)]\ ]$. In this convolution $p1$ is a familiar object, so all of cp_1*'s* novel properties must stem from $\mathbf{FT}^{-1}[Sign[jinc(q)]$. That function is not known analytically, but its general form can be discerned from computation and comparison with known spectra for similar functions. Fig. 10 shows $\mathbf{FT}^{-1}[Sign[jinc(q)]$ computed by numerical integration using an upper limit of q = 10. Its main feature is a pair of positive and negative rings located just inside and outside radius r = 0.5. In profile (Fig. 10*e*) these rings look like low-pass versions of positive and negative ring-impulses: radial delta-functions of the form $+\delta(r - .5+\varepsilon))$ and $-\ \delta(r -.5-\varepsilon)$, where ε is some small value << .5. Increasing the upper limit of integration enhances this impulse-ring quality, and drives ε towards zero, suggesting that the limit of the full integration will be something close to the radial dipole $\delta'(r-.5)$. That object is essentially a pair of + and – ring impulses with ε = 0.

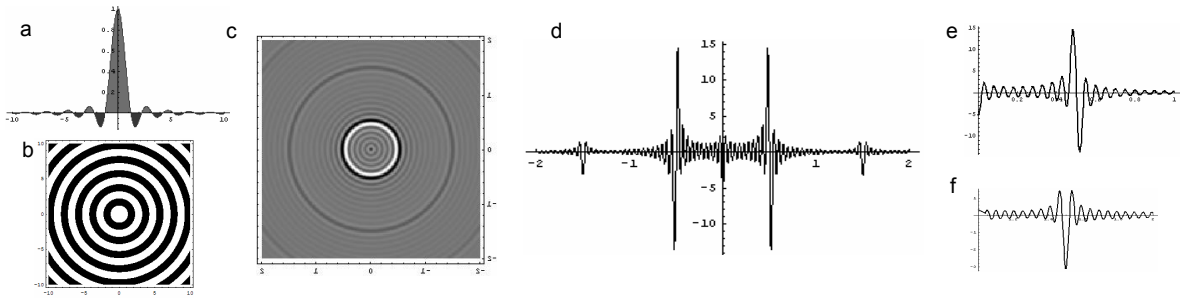

Fig. 10 *a*: $(4/\pi)\ jinc(q)$ (profile) *b:* $Sign[jinc(q)]$ (top view) c: $\mathbf{FT}^{-1}[\ Sign[jinc(q)]\ ]$ (top view)
d: $\mathbf{FT}^{-1}[\ Sign[jinc(q)\ ]$ (profile) *e:* blowup of $\mathbf{FT}^{-1}[Sign[jinc]]$ at its first ring *f:* blowup at second ring

That expectation is supported by comparison with the closely related radially periodic function *Sign[sinc(q)] = Sign[sin πq/πq] = Sign[sin π|q|]*. The analytic form of the **FT** of this function has been derived by Amidror[13,14], who shows that its main feature is an impulsive dipole-like ring of the form $\delta^{(1/2)}(r-.5)$, i.e., a half-order derivative impulse-ring at $r = 0.5$. Amidror's generalized function analysis of periodic radial functions cannot be directly applied to *Sign[jinc(q)]*, which is not (quite) periodic. But computational comparisons (see Fig. 11) indicate that these two **FT**s have essentially the same form out through the critical first ± impulse-ring pair, and differ only in the exact shape of those impulses. This leaves little doubt that the limit for $\mathbf{FT}^{-1}$[*Sign[jinc(q)]*] will be dominated by an impulsive radial dipole of the general form $\delta^{(\lambda)}(r-.5)$, with λ in the range ½ to 1. Finding an exact generalized function representation for this fundamental object is an interesting open problem. With that function in hand, convolution with the uniform disk p1(r) would provide an exact expression for the phase-corrected pointspread function *cp1(r)*. (We have obtained an exact result of this sort for the case of defocus with a square pupil. There the role played by the half-order deriviative $\delta^{(1/2)}(r-.5)$ in the spectrum of *Sign[sinc(q)]* falls instead to the 1-dimensional Hilbert transform of *δ(x-.5)*--another kind of approximate derivative.)

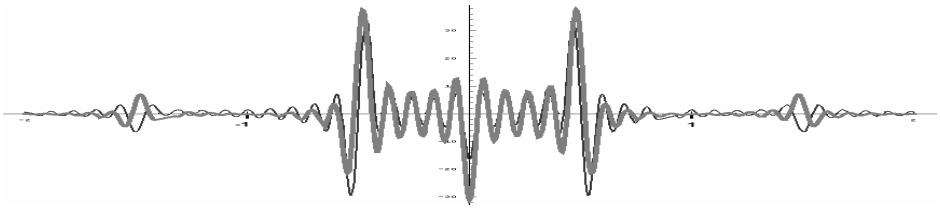

Fig. 11. $\mathbf{FT}^{-1}$[*Sign[jinc(q)]*](*r*) (thin line) versus $\mathbf{FT}^{-1}$[*Sign[sinc(q)]*](*r*) ; $-2 \le r \le 2$

But even without an exact expression for $\mathbf{FT}^{-1}$[*[Sign[jinc(q)]*](r) , we can be confident that in its convolution with *p1*(r), this function will act essentially like a pair of positive and negative impulse rings located just inside and just outside the circle $r = 0.5$. This allows us to understand how the SR-corrected pointspread *cp1* gets its characteristic form. Figure 11 illustrates the process. The basic effect is that the positive impulse ring with radius 0.5−ε creates an annulus of overlapping positive-value unit-diameter disks, all centered on the circle $r = 0.5-\varepsilon$. The negative impulse ring (with radius 0.5+ε) creates a second annulus composed of overlapping negative-value unit-diameter disks centered on the circle $r = 0.5+\varepsilon$. These positive and negative annuli add together to cancel one another everywhere, except for a small intensely positive spot at the origin, where all of the positive disks overlap and there is no negative cancellation, and a thin negative annulus with radius ~1.0,where the outer rims of the negative disks add together uncancelled, and produce a ring of negative light-intensities. This accounts for the two characteristic properities of SR-corrected pointspread functions: a sharp impulsive spike at the origin, and a negative ring whose radius is the diameter of the blur-disk.

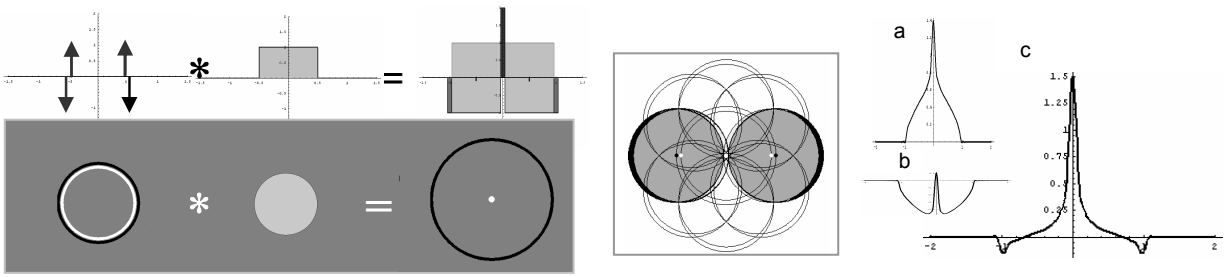

Fig. 12. Effect of convolving positive and negative impulse-rings with a uniform disk. The *top-left* series illustrates the idea in 1-D: Convolving *rect(x)* with $\delta(x-.5+\varepsilon) - \delta(x-.5-\varepsilon)) + (\delta(x+.5-\varepsilon) - \delta(x+.5+\varepsilon)$ (here $\varepsilon = .05$) creates a positive pulse with amplitude +2 at $x = 0$, and negative pulses with amplitude -1 at $x = \pm 1$. The *bottom-left* series illustrates the analogous operation in 2-D: convolving a uniform disk with a pair of impulse rings $\pm \delta(r - .5 \pm \varepsilon)$. The *center figure* schematizes the effect of adding partially-overlapping positive and negative disks. *Figures a-c* on the right show profiles of the functions created by *(a)* convolving a unit-diameter disk with the positive impulse ring $+\delta(r-.5+\varepsilon)$; *(b)* convolving the disk with a negative ring $-\delta(r-.5-\varepsilon)$; (*c)* adding *a* and *b*. This creates a sharp spike at the origin and a negative annulus at $r = 1$, reproducing the basic form of the SR corrected pointspread function shown in Fig. 8.

4. PRE-CORRECTING SPURIOUS RESOLUTION

Our analysis so far has dealt with correcting SR in an image i_o that has already been defocused by a known pointspread function p ($i_o = o * p$), and is available in a form that allows us compute its spectrum Fi_o ($= Fo\ Tp$), correct the phase errors in that spectrum ($Fci_o = Fi_o\ Sign[Tp]$), and invert the result to produce a corrected image ($ci_o = \mathbf{FT}^{-1}[Fci_o]$) which still suffers the contrast-loss imposed by defocus, but has a perfect phase spectrum ($Fci_o = |Fo|\ |Tp|\ exp[j\Phi_o]$). We have seen that this operation can greatly improve the recognizability of objects defocused by amounts that commonly occur in presbyopic vision (Figs. 6,7). Of course there the defocused image that needs correction is on the retina, beyond our reach. But as noted in Sec. 1, we can still hope to repair its phase errors by correcting them in advance, using the mathematical fact that $Sign[Tp]$ in the product $(Fo\ Tp)\ Sign[Tp] = Fci_o$ can just as well be inserted in the order $(Fo\ Sign[Tp])\ Tp = Fci_o$. So if we could create the pre-corrected object $co = \mathbf{FT}^{-1}[Fo\ Sign[Tp]]$, its retinal image would be $\mathbf{FT}^{-1}[Fo\ Sign[Tp]\ Tp] = \mathbf{FT}^{-1}[\ Fci_o] = ci_o$, the same image created by post-defocus SR-correction. In that case the same improvement in image quality produced by correcting SR in defocused images of letters could be achieved by pre-correcting the letters themselves.

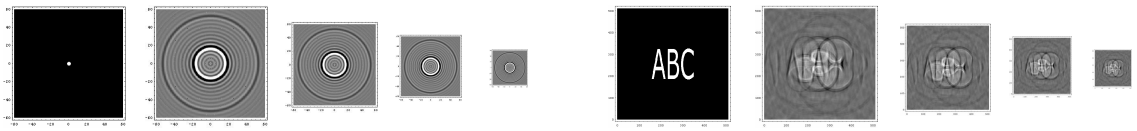

Fig.13 Images pre-corrected for spurious resolution. Left series: point object $\delta(r)$ and its pre-corrected version $c\delta(r)$ at four magnification levels. Right series: pre-corrected images of the letters used in Fig. 6.

The problem with this scheme is that the mathematical object $co(x,y)$ created by the operation $\mathbf{FT}^{-1}[Fo\ Sign[Tp]]$ will generally not be a physically possible image, and the changes required to turn it into one have the effect of greatly reducing the contrast of the final image (i.e., the retinal image) that results after optical defocus. Figure 13 shows sample results: pre-corrected versions of a point, and of the letters whose SR-correction was illustrated in Fig. 6. These images might be expected to look like low-contrast points and letters after sufficient defocus (i.e., if viewed sufficiently close up. Several magnifications are included to facilitate observations with printed copies) With a little visual exploration, the point image seems to work fairly well. The visual impression it gives is one of a fuzzy low-contrast white point on a roughly uniform gray background, much like panel 9 in Fig. 14 below. (The letters also can become faintly visible, but this requires a more sympathetic eye.) That figure illustrates why SR pre-correction followed by defocused imaging creates a lower contrast physical image than the one produced by

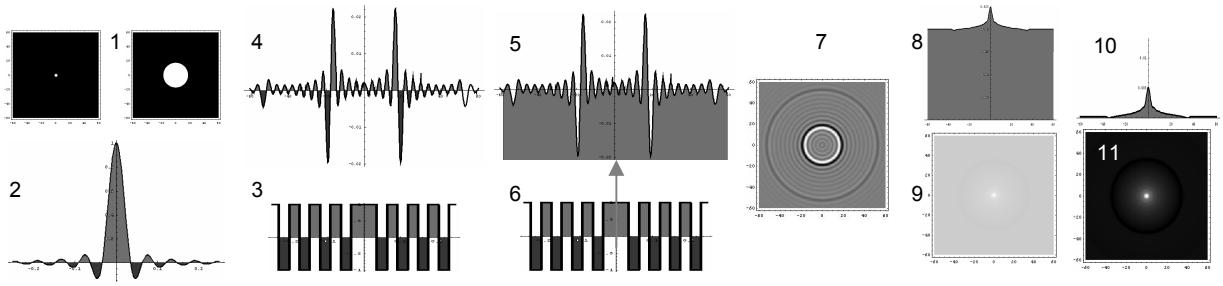

Fig. 14 Effect of pre-correcting a point for spurious resolution using the model eye from Fig.2. *Panel 1*: point object $o = \delta$ and uniform-disk pointspread p *2*: OTF $Tp(q)$ *3*: $Sign[Tp(q)]$ *4*: $\mathbf{FT}^{-1}[Sign[Tp]]$ (This is $c\delta$ when $Tp(q)$ is low-pass filtered to $q \leq 15$ cycles/deg.) 5: $c\delta$ made nonnegative by adding a constant $M = |\mathrm{Min}[c\delta\ ]|$. *6*: spectrum of $c\delta + M$ *7*: Top view of $c\delta + M$. Defocusing this image should produce a retinal version of the SR-corrected image of a point. (For 3 diopter defocused viewing at 30 cm with a 3 mm pupil, the white-black ring radius should be 1.5 mm.) Panels *8* and *9*: image $c\delta + M$ after defocus (i.e., after convolution with p); profile and top view. This is the retinal image of the pre-corrected point. *Panels 10* and *11* show the image produced by correcting SR post-defocus (i.e., $\mathbf{FT}^{-1}[|Tp|]$). Its peak/background intensity ratio is 16.7 vs. 1.3 for the image in panels 8,9.

correcting SR in an image that has already been defocused. (Fig. 14-11 shows the comparable post-defocus SR-corrected image, i.e., $\mathbf{FT}^{-1}[|Tp|]$ obtained with the same parameters that produce 14-9 when used in pre-correction.) The object here is a point $\delta(x,y)$ viewed at 30 cm by the model presbyopic eye analyzed earlier in Sec. 2 (Figs. 2 and 3). Defocused imaging is modeled by convolution with a uniform disk $p(r) = (4/\pi D^2)\ rect(r/D)$, with diameter D = 33 min. The OTF is $Tp(q) = (4/\pi)\ jinc(Dq)$. The theoretical SR pre-corrected point $c\delta(r)$ is $\mathbf{FT}^{-1}[\ Sign[Tp]\ ](r) = \mathbf{FT}^{-1}[Sign[jinc(Dq)]](r)$. That function cannot be directly represented as a physical image, for two reasons: it has infinite values (because it consists of a set of ring impulses), and it has negative values (in particular, the dominant ring-impulse pair at r = D/2 has the form $\pm\ \delta(r - (D/2) \pm \varepsilon)$). Infinite values do not pose a fundamental problem, because Tp in reality always incorporates low-pass filtering by diffraction at the pupil (not to mention limits imposed by printing or video display), so we always have effectively $Tp(q) = Tp(q)\ rect(q/2q_{max})$ for some cutoff frequency q_{max}. This means that our infinite ring-impulses are really finite functions of the form $(2q_{max})^2\ jinc(r/2q_{max}) * \pm\ \delta(r - (D/2) \pm \varepsilon)$. (Fig. 14-4 shows the filtered version of $c\delta(r)$ produced by q_{max} = .25 cycles/min.) But this still leaves a function whose negative values are as large as its positive values. To make this object into a physical image, we have to add a constant M large enough to cancel its most negative value. This creates an entirely positive,and thus imagable, function, like the profile shown in Fig. 14-5. Fig. 14-7 shows the corresponding image; 14-6 is the profile of its spectrum (which is $Sign[Tp]\ rect(q/2q_{max}) + M\delta(u,v)$). When this physical version of the pre-corrected object $c\delta$ is imaged by a presbyopic eye (i.e., when its spectrum is multiplied by Tp), the added DC level M passes through the imaging process unattentuated, and acts like a veiling light: the retinal image will be $\mathbf{FT}^{-1}[|Tp(q)|\ rect(q/2q_{max})](r) + M$. Here the $\mathbf{FT}^{-1}$ part is the sharply peaked pointspread function that results from correcting SR in a defocused filtering image (e.g., Fig. 8, and here in Fig. 14-10,11), and M is always a relatively large constant that dwarfs the rest of the function, giving the entire image uniformly low contrast (as shown in Fig. 14-8,9).

Such low-contrast (but phase-perfect) images seem to be the best we can expect from phase-only reading glasses. The problem stems from the essential nature of SR-correction, based as it is on the cancellation of equally large positive and negative light intensities, as we saw in Sec. 3.3. It seems to impose a fundamental limit on the visual improvement that can be expected from pre-correcting phase alone in objects destined for out-of-focus viewing. Progress along this line can perhaps be made by pre-correcting spectral amplitude as well as phase.

REFERENCES

1. G. Smith,"Optical defocus, spurious resolution, and contrast reversal," *Ophthal. Physiol. Opt.* 2(1), 5-23 (1982).
2. J. Goodman, *Introduction to Fourier Optics,* McGraw-Hill, San Francisco, 1968.
3. G. Smith and D.A. Atchison, *The Eye and Visual Optical Instruments,* Cambridge University, Cambridge, 1997.
4. A. Leonova, J.S. McLellan, and S.A. Burns, "Do optical phase reversals affect perception of natural scenes?" *Journal of Vision* 4(11). 62a (2004).
5. G. Legge, K.T. Mollen, G.C.Woo, and F.W. Campbell, "Tolerance to visual defocus," *J. Opt. Soc. Am. A* 4(5), 851-863 (1987) .
6. D.A. Atchison, R.L. Woods, and A. Bradley, "Predicting the effects of optical defocus on human contrast sensitivity," *J. Opt. Soc. Am. A* 15(9), 2536-2544 (1998).
7. S. Ravikumar, A. Bradley, L. Thibos, and X. Cheng, "The visual impact of phase and amplitude changes in optically aberrated images," *Investigative Ophthalmol. Vis. Sci.* 46:E-Abstract 2012 (2005)
8. G.E Legge, D.G. Pelli, G.S.Rubin, and M.M.Schleske, "Psychophysics of reading--I. Normal vision," *Vision Res.* 25(2), 239-252 (1985).
9. H.H. Hopkins, 'The frequency response of a defocused optical system," *Proc. Roy. Soc. A* 231(1184), 91-103 (1955).
10. P. Stokseth, "Properties of a defocused optical system," *J. Opt. Soc. Am.* 59(10), 1314-1321 (1969).
11. R.A. Applegate, "Wavefront sensing, ideal corrections, and visual performance," *Optometry and Vision Science* 81(3), 167-177.
12. R.N. Bracewell, *Fourier Analysis and Imaging,* Kluwer Academic/Plenum Publishers, New York, 2003.
13. I. Amidror, "Fourier spectrum of radially periodic images," *J. Opt. Soc. Am. A* 14(4), 816-826 (1997).
14. I. Amidror, "Fourier spectra of radially periodic images with a non-symmetric radial period," *J. Opt. A: Pure Appl. Opt*. 1, 621-625 (1999).